International Journal of Environmental Sciences
ISSN: 2229-7359
Vol. 11 No. 21s, 2025
https://theaspd.com/index.php

Geant4-Based Simulation Of Charged Particle Deflection In Magnetic Fields For Beam Profiling In Proton And Electron Therapy

Hanan Akhdar[1], Maha Algarawi[1], Hanan Aleidan[1], Joud Aleready[1], Razan Almokhalifi[1], Nojoum Majrabi[1]
[1]Department of Physics, Faculty of Science, Imam Mohammad Ibn Saud Islamic University (IMSIU), P.O. Box 90950, Riyadh 11623, Saudi Arabia
Hanan.akhdar@gmail.com; mmgarawi@imamu.edu.sa; 441019127@sm.imamu.edu.sa; 444008333@sm.imamu.edu.sa; 442021679@sm.imamu.edu.sa; 442012277@sm.imamu.edu.sa.
*Corresponding Author: Hanan.akhdar@gmail.com

Abstract– *Proton and electron therapy, offer advanced treatment options due to their precision in dose localization and ability to spare healthy tissues. This study investigates the deflection behavior and energy deposition profiles of electron and proton beams under transverse magnetic fields using Geant4 toolkit. Simulations were conducted using water phantoms embedded with tumors at shallow (1 cm), medium (5 cm), and deep (10 cm) depths. Electron beams (5–20 MeV) and proton beams (6–250 MeV) were analyzed under varying magnetic field strengths (up to 0.03 T for electrons and 0.3 T for protons). Energy deposition was scored in pre-tumor, tumor, and post-tumor regions. Geant4 results were validated against theoretical deflection angles derived from Lorentz force calculations. The results underscore the importance of tailoring charged particle therapy to tumor depth and location. Electron therapy is best suited for superficial tumors, while proton therapy offers superior spatial control for deep or anatomically complex targets.*

Keywords– *Geant4, Proton therapy, Electron therapy, Magnetic field deflection, Radiation dose distribution, Tumor depth optimization.*

I. INTRODUCTION

Radiation therapy is an important approach in cancer treatment, especially when employing advanced techniques such as proton therapy and electron therapy, which uses charged particle beams for high precision in tumor targetting and minimal normal tissue exposure. These techniques are shaped by the physical interactions of the particles with matter, as well as external influences like magnetic fields.

1.1 Proton Beam Radiation Therapy

The therapeutic potential of proton depth-dose characteristics was initially recognized in a report by Wilson in 1946, wherein he theorized the application of proton beams for the treatment of localized cancers. The first patient was treated using protons in 1954 at the University of California, Berkeley. Over time, facilities like the Harvard Cyclotron Laboratory and research centers in Sweden, Russia, and Japan contributed significantly to the field [1].

Proton therapy is distinguished by its Bragg peak—a sharp rise in dose at a defined depth followed by rapid falloff—allowing for precise delivery to tumors while sparing surrounding tissues. This enables safer treatment of tumors near critical organs [1–4]. Proton beams of 60–250 MeV deposit most of their energy at the tumor site, with negligible exit dose, which makes the technique particularly effective for pediatric and skull base tumors [2].

The interactions governing proton behavior include Inelastic Coulomb interactions with electrons, Elastic Coulomb scattering with nuclei, and Nuclear reactions which may produce secondary particles [5].

1.2 Electron Beam Radiation Therapy

Although photons have historically been the primary modality for radiation therapy, electrons are preferred in certain cases due to their physical properties, particularly their limited penetration depth in tissue [6].

Electron therapy is commonly used for shallow tumors, including skin, chest wall, and head-and-neck lesions. Electrons deposit energy rapidly within the first few centimeters of tissue and are highly scatter-

prone. Their dose distribution is flatter at shallow depths, making them ideal for surface-level therapy because it protects deeper healthy tissues [6].

Due to their lower mass, electrons are significantly more sensitive to magnetic field deflection than protons. Even small magnetic field strengths can cause trajectory distortion, which impacts both treatment precision and safety [6,7].

1.3 Magnetic Field Effects in Charged Particle Therapy

Charged particles generally travel in straight lines, but when they pass through a magnetic field, they are deflected by the Lorentz force. This deflection is circular and depends on the particle's charge, speed, and mass, as well as the magnetic field strength. This principle applies to both protons and electrons, though its effect is greater on electrons [8,9].

The relationship between deflection angle and magnetic field is key in MR-guided therapies and must be quantified to avoid unintended beam deviation [9]. Precise control of the magnetic field can also be used to steer the beam and improve dose localization [10].

1.4 Geant4 Simulation Toolkit

Geant4 is an open-source simulation toolkit designed to model the passage of particles through matter. Developed using object-oriented C++, it includes modules for geometry construction, particle tracking, event handling, and a wide range of physical processes [11].

Geant4 is widely used in medical physics, space science, and nuclear engineering for its versatility and high fidelity in simulating radiation transport [11].

1.5Aim of the Study

This research aims to investigate the influence of magnetic fields on the deflection and energy deposition of proton and electron beams using Geant4 simulations. The first step is the validation of the simulation output against theoretical deflection derived from Lorentz force equations. The second step is the evaluation of different treatment scenarios at shallow, medium-depth, and deep tumors using clinically relevant energies and magnetic field strengths. Finally, recommending optimized therapy parameters for each modality based on dose localization and magnetic influence.

II. MATERIALS AND METHODS

2.1Simulation Environment

Simulations were conducted using the Geant4 toolkit, applying its electromagnetic physics list for both proton and electron interactions. The geometry included a water phantom measuring 20 × 20 × 20 cm^3 with a soft-tissue-equivalent tumor volume (G4_TISSUE_SOFT_ICRP) positioned at 1 cm depth to represent a shallow tumor, 5 cm depth to represent a medium depth tumor and 10 cm depth to represent a deep tumor.

Three scoring regions were defined: pre-tumor, tumor, and post-tumor, to record energy deposition in each layer. A uniform magnetic field was applied in the positive Y direction, perpendicular to the beam axis (Z-direction), consistent with the experimental layout [9].

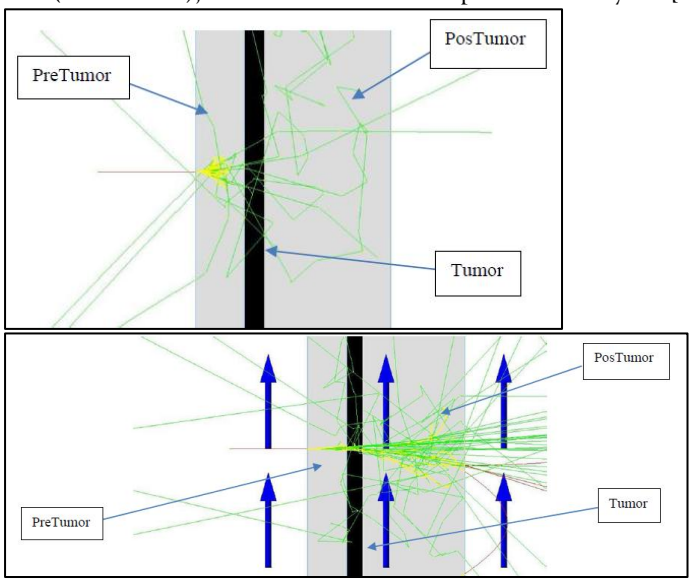

Figure 1. The water phantom with the tumor placed within and the beam interactions in the Geant4 simulation (top). Magnetic field direction with the water phantom and tumor in the Geant4 simulation (bottom).

2.2 Beam Configurations

In this study, both proton and electron therapy were simulated using clinically relevant beam and field parameters. Proton beams were modeled with energies ranging from 60 to 250 MeV, while electron beams ranged from 5 to 20 MeV. To investigate the influence of external magnetic fields, protons were subjected to fields between 0.1 and 0.3 Tesla, whereas electrons, due to their higher sensitivity to magnetic deflection, were tested under weaker fields ranging from 0.01 to 0.03 Tesla. For both particle types, the simulations focused on analyzing key output metrics, including the total energy deposited (Edep) in various regions of the phantom, the deflection angle, and the resulting radius of curvature of particle trajectories.

2.3 Validation of Geant4 Accuracy

To ensure accurate simulation, deflection angles were calculated theoretically using the Lorentz force as in equation (1):

$$F = qvB, r = \frac{mv}{qB}, \theta = \frac{L}{r} \quad (1)$$

Where F is Lorentz force, B is the magnetic field applied, m is the mass of the charged particle passing through the magnetic field, q is its charge, θ is the angle of deflection due to the magnetic field, r is the radius of curvature, L is the path length and v is the velocity which is also computed using relativistic energy as in equation (2) stated [12,13,14]:

$$v = c\sqrt{1 - \left(\frac{m_0 c^2}{E}\right)^2} \quad (2)$$

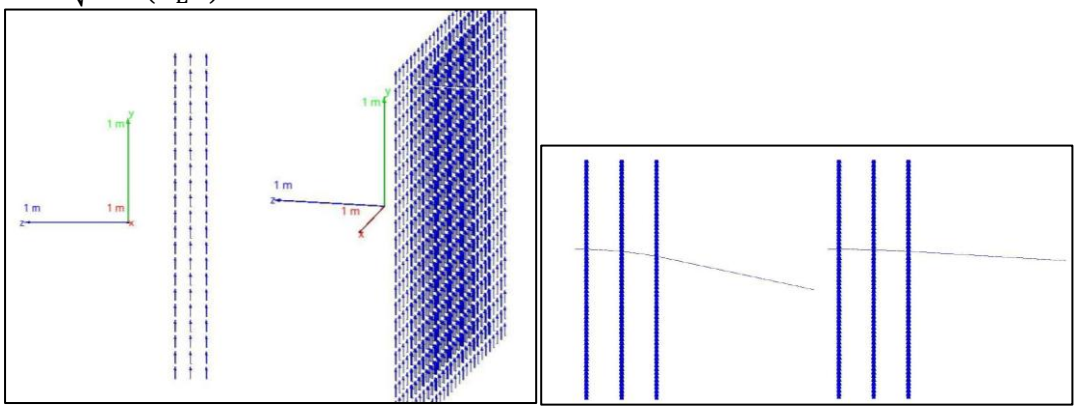

Figure 2. Magnetic field direction in the Geant4 simulation (left). Deflection of charged particles due to the magnetic field in the Geant4 simulation (right).

Geant4 angles were obtained from momentum vectors before and after the deflection as in equation (3) [11]:

$$\cos\theta = \frac{\vec{P}_{initial} \cdot \vec{P}_{final}}{|\vec{P}_{initial}||\vec{P}_{final}|} \quad (3)$$

The percentage error was calculated as in equation (4):

$$Error\% = \frac{|\theta_{experimental} - \theta_{theoratical}|}{\theta_{theoratical}} \quad (4)$$

Both electron and proton validation results showed acceptable errors, confirming the accuracy of the simulations [14].

2.4 Energy Deposition and Dose Analysis

After validation, energy deposition was scored in each region of the phantom under varying particle energies, magnetic field strengths and tumor positions inside the water phantom. For each scenario, the percentage of total deposited energy within the tumor region was calculated and plotted. Trends were analyzed with respect to both particle type and treatment configuration.

III. RESULTS

3.1 Shallow Tumor

Table 1 shows the collected data from Geant4 in case of shallow tumor of thickness 2 cm placed 1 cm away from the surface of a water phantom.

TABLE 1. SHALLOW TUMOR SIMULATION RESULTS.

Shallow Tumor							
Magnetic Field (Tesla)	Beam Energy (MeV)	Pre-Tumor Energy Deposit (MeV)	Tumor Energy Deposit (MeV)	Post-Tumor Energy Deposit (MeV)	Deflection Angle (degree)		Tumor Percentage Energy Deposit (%)
					Mean	SD	
Electron Therapy							
0	5	991.7370	85.2993	8.9582	0.0092	1.0542	7.85%
	10	892.7800	1040.3300	175.4450	0.0110	1.1301	49.34%
	15	834.9920	1048.2300	1221.7600	0.0108	1.1047	33.76%
	20	828.8370	972.8860	2222.8600	0.0122	1.1662	24.17%
0.01	5	991.9790	86.5120	8.9361	0.0099	1.0788	7.96%
	10	897.0130	1040.4600	169.2550	0.0100	1.0565	49.39%
	15	833.5900	1045.3100	1209.0800	0.0102	1.0706	33.85%
	20	825.0670	975.0510	2203.1100	0.0113	1.1120	24.36%
0.02	5	997.1060	80.5258	10.2964	0.0091	1.0549	7.40%
	10	897.8510	1040.2200	168.2790	0.0105	1.0840	49.38%
	15	835.3270	1053.2200	1203.4100	0.0110	1.1282	34.06%
	20	831.2860	980.0660	2223.7800	0.0123	1.1765	24.29%
0.03	5	999.1640	77.0204	10.7952	0.0102	1.1093	7.09%
	10	906.9670	1034.4800	165.4500	0.0112	1.1291	49.10%
	15	837.4800	1056.5400	1200.1500	0.0119	1.1601	34.15%
	20	829.8480	980.4910	2204.8600	0.0110	1.0914	24.42%
Proton Therapy							
0	6	6912.3000	9424.5900	0.0246	0.0000	0.0656	57.69%
	120	3320.3600	3979.3900	24570.4000	0.0000	0.0444	12.49%
	180	2394.3700	2681.8200	29968.5000	0.0002	0.0998	7.65%
	250	1897.9000	2081.7100	17657.6000	0.0002	0.1044	9.62%
0.1	6	6910.9600	9423.0800	0.0218	0.0000	0.0238	57.69%
	120	3318.3800	3982.5400	24572.4000	0.0000	0.0379	12.49%
	180	2395.1700	2683.0200	29969.5000	0.0001	0.0398	7.66%
	250	1897.9500	2081.5700	17657.0000	0.0001	0.0698	9.62%
0.2	6	6912.7500	9421.6100	0.0000	0.0000	0.0159	57.68%
	120	3321.4000	3979.9500	24576.5000	0.0000	0.0264	12.49%
	180	2395.4700	2682.4800	29983.4000	0.0001	0.0657	7.65%
	250	1897.6000	2083.6500	17663.1000	0.0002	0.0876	9.63%
0.3	6	6914.2600	9421.5900	0.0091	0.0000	0.0242	57.67%
	120	3321.4200	3982.6800	24565.8000	0.0000	0.0307	12.50%
	180	2392.5100	2681.5300	30012.5000	0.0001	0.0530	7.64%
	250	1898.1900	2083.5400	17668.5000	0.0002	0.0702	9.62%

As shown in the figures 3-6, at shallow depths, electron therapy demonstrated highly favorable dose localization, with tumor energy deposition peaking at 1056.54 MeV for a 15 MeV beam under 0.03 T field conditions. The average tumor energy deposition across all shallow electron cases was approximately 787.29 MeV, with a minimum of 77.02 MeV observed at lower beam energies.

The highest tumor percentage (up to ~49%) was achieved at 10 MeV, after which energy deposition declined due to deeper penetration and increased scattering. Pre-tumor regions consistently absorbed higher doses at low energies, while post-tumor doses remained minimal, confirming effective beam fall-off in shallow setups.

International Journal of Environmental Sciences
ISSN: 2229-7359
Vol. 11 No. 21s, 2025
https://theaspd.com/index.php

Magnetic fields up to 0.03 T had limited influence on tumor dose percentages but affected deflection angles, increasing lateral spread. However, the mean deflection angles remained below 0.0123°, confirming manageable geometric accuracy for this energy range.

On the other hand, Proton therapy at shallow tumor depths showed a contrasting pattern. Low-energy protons (6 MeV) delivered very high tumor doses (~9424.6 MeV) with minimal exit dose, consistent with Bragg peak characteristics. However, higher-energy protons (e.g., 120–250 MeV) penetrated too deeply, resulting in lower tumor deposition percentages (as low as ~7.6%).

Notably, the average tumor energy deposition for shallow proton therapy was 4542.17 MeV, about 5.8× greater than electron therapy, emphasizing their superior penetration power but also underlining the risk of overtreatment beyond shallow depths.

Magnetic fields of 0.1–0.3 T reduced the proton beam deflection significantly (angle range ~0.0001° to 0.0091°), ensuring excellent trajectory control. This makes protons particularly well-suited for MR-guided or magnetically collimated systems.

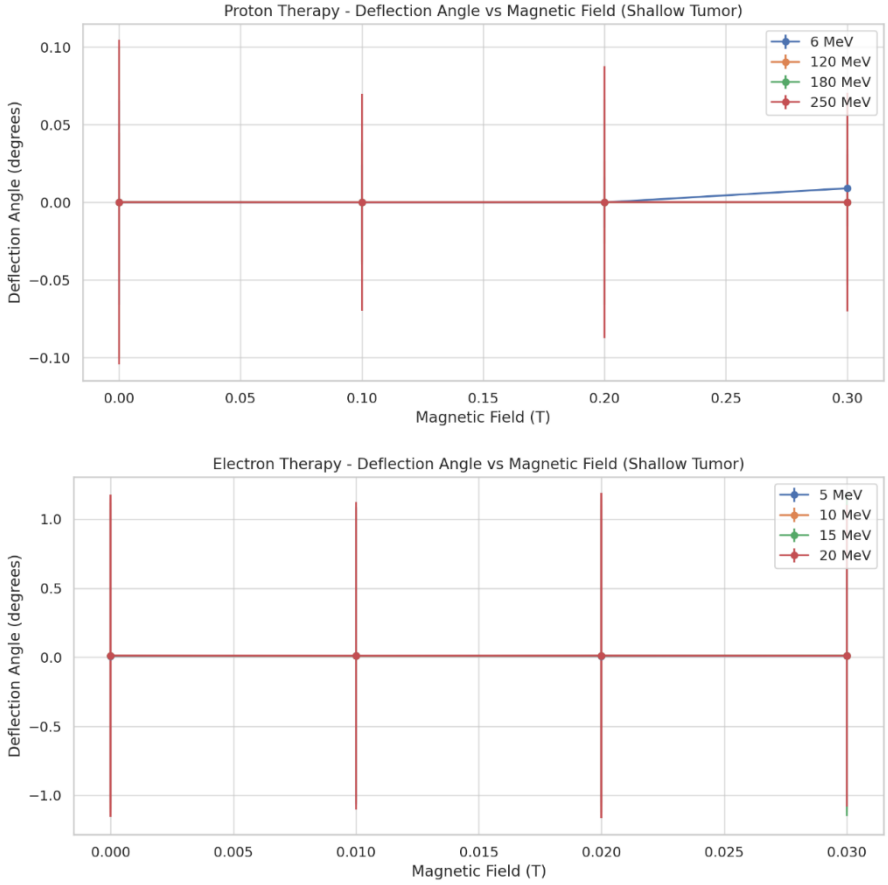

Figure 3. Deflection angle vs magnetic field in the shallow tumor simulation. In case of proton therapy (top) and electron therapy (bottom).

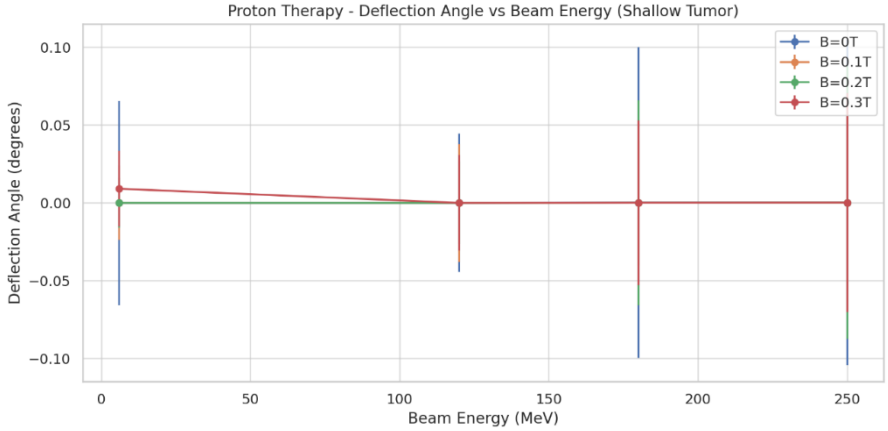

International Journal of Environmental Sciences
ISSN: 2229-7359
Vol. 11 No. 21s, 2025
https://theaspd.com/index.php

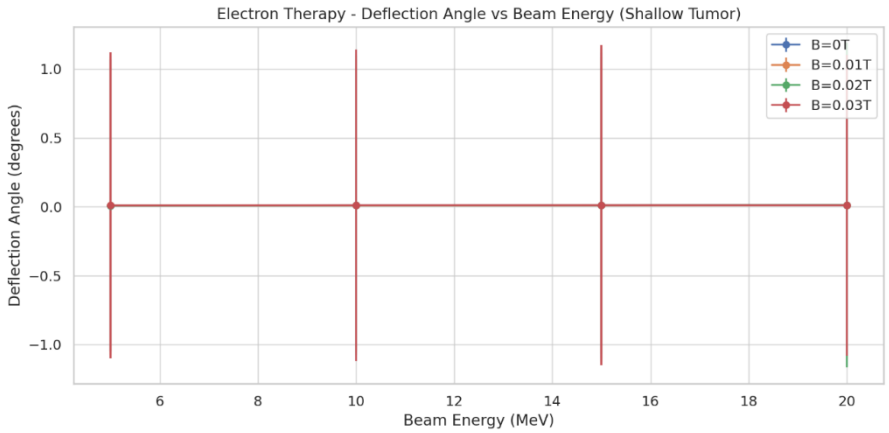

Figure 4. Deflection angle vs beam energy in the shallow tumor simulation. In case of proton therapy (top) and electron therapy (bottom).

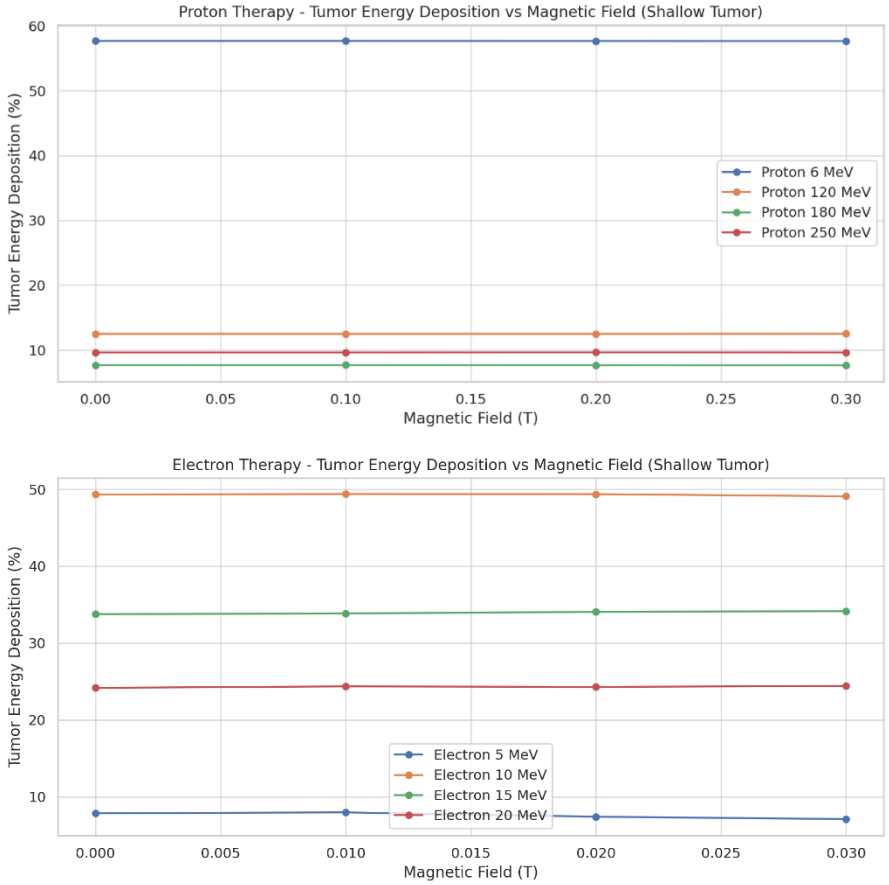

Figure 5. Tumor energy deposition vs magnetic field in the shallow tumor simulation. In case of proton therapy (top) and electron therapy (bottom).

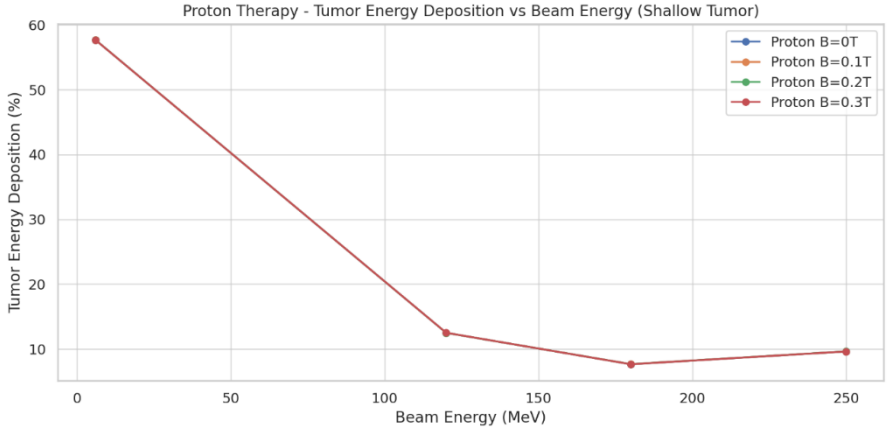

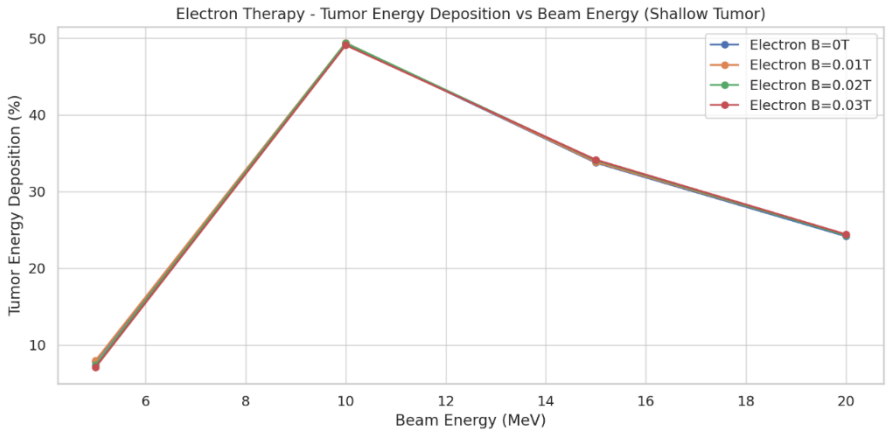

Figure 6. Tumor energy deposition vs beam energy in the shallow tumor simulation. In case of proton therapy (top) and electron therapy (bottom).

3.2 Medium-depth Tumor

Table 2 shows the collected data from Geant4 in case of medium depth tumor of thickness 2 cm placed 5 cm away from the surface of a water phantom.

TABLE 2. MEDIUM-DEPTH TUMOR SIMULATION RESULTS.

Medium-depth Tumor							
Magnetic Field (Tesla)	Beam Energy (MeV)	Pre-Tumor Energy Deposit (MeV)	Tumor Energy Deposit (MeV)	Post-Tumor Energy Deposit (MeV)	Deflection Angle (degree) Mean	SD	Tumor Percentage Energy Deposit (%)
Electron Therapy							
0	5	4.9400	1075.6400	2.2590	0.0091	1.0300	99.34%
	10	28.9205	2055.9100	15.0184	0.0101	1.0622	97.91%
	15	96.7224	2303.4500	706.7390	0.0109	1.1170	74.14%
	20	791.4090	2213.2500	991.6750	0.0110	1.0939	55.38%
0.01	5	5.1253	1077.3900	1.8195	0.0080	0.9413	99.36%
	10	26.6430	2058.8300	14.9576	0.0100	1.0591	98.02%
	15	91.0740	2300.8100	710.4260	0.0105	1.0798	74.16%
	20	793.3630	2210.5200	984.9110	0.0115	1.1244	55.42%
0.02	5	6.9469	1075.6600	1.5616	0.0080	0.9557	99.22%
	10	26.6706	2057.7100	13.9004	0.0101	1.0685	98.07%
	15	84.2605	2302.8300	714.0640	0.0116	1.1409	74.26%
	20	806.9120	2210.4200	989.6310	0.0114	1.1178	55.16%
0.03	5	7.6719	1075.4400	2.8184	0.0094	1.0541	99.03%
	10	31.9753	2056.2300	15.0037	0.0106	1.0927	97.77%
	15	85.3138	2305.4200	701.5270	0.0109	1.1132	74.55%
	20	791.9690	2215.3000	998.6220	0.0107	1.0797	55.30%
Proton Therapy							
0	6	0.0000	16654.2000	0.0000	0.0000	0.0574	100.00%
	120	17808.1000	9026.4800	5013.8300	0.0000	0.0433	28.34%
	180	25972.8000	6191.3100	2901.4900	0.0002	0.0881	17.66%
	250	14671.5000	4825.5700	2156.1500	0.0002	0.0878	22.29%
0.1	6	0.0000	16654.2000	0.0000	0.0000	0.0574	100.00%
	120	17808.1000	9026.4800	5013.8300	0.0000	0.0433	28.34%
	180	25972.8000	6191.3100	2901.4900	0.0002	0.0881	17.66%
	250	14671.5000	4825.5700	2156.1500	0.0002	0.0878	22.29%

0.2	6	0.0000	16654.3000	0.0000	0.0000	0.0226	100.00%
	120	17806.0000	9027.5100	5014.2200	0.0000	0.0272	28.35%
	180	26000.8000	6192.1900	2905.3100	0.0001	0.0592	17.64%
	250	14672.1000	4826.9400	2157.7300	0.0001	0.0523	22.29%
0.3	6	0.0000	16654.2000	0.0000	0.0000	0.0226	100.00%
	120	17799.7000	9027.8500	5015.5200	0.0000	0.0263	28.35%
	180	26021.5000	6191.8800	2904.5000	0.0001	0.0605	17.63%
	250	14677.3000	4822.5400	2155.1100	0.0002	0.0671	22.27%

As shown in figures 7-10, electrons at medium depths retained excellent tumor targeting at lower beam energies (5–10 MeV) with tumor deposition percentages reaching 99.36% under 0.01 T. However, higher energies led to deeper penetration and increased scatter, resulting in significant post-tumor dose (e.g., 706.74 MeV at 15 MeV).

Magnetic field increments had negligible effects on tumor dose percentages (variation ≤0.5%) but influenced deflection angles, reaching up to 0.0116° at 15 MeV. This indicates minimal lateral drift, affirming geometric suitability for medium-depth treatments.

Protons at medium depths (6–250 MeV) showed improved performance at 120 MeV, where a substantial tumor dose (˜9026 MeV) was achieved with post-tumor deposition controllable via magnetic field tuning. However, deep-seated Bragg peaks from higher energies (e.g., 180–250 MeV) caused increased exit dose. Tumor energy percentages dropped to ˜17–28% at these higher energies due to overshooting the medium target. Magnetic deflection remained tightly confined (<0.0002°), even at 0.3 T fields, demonstrating excellent spatial

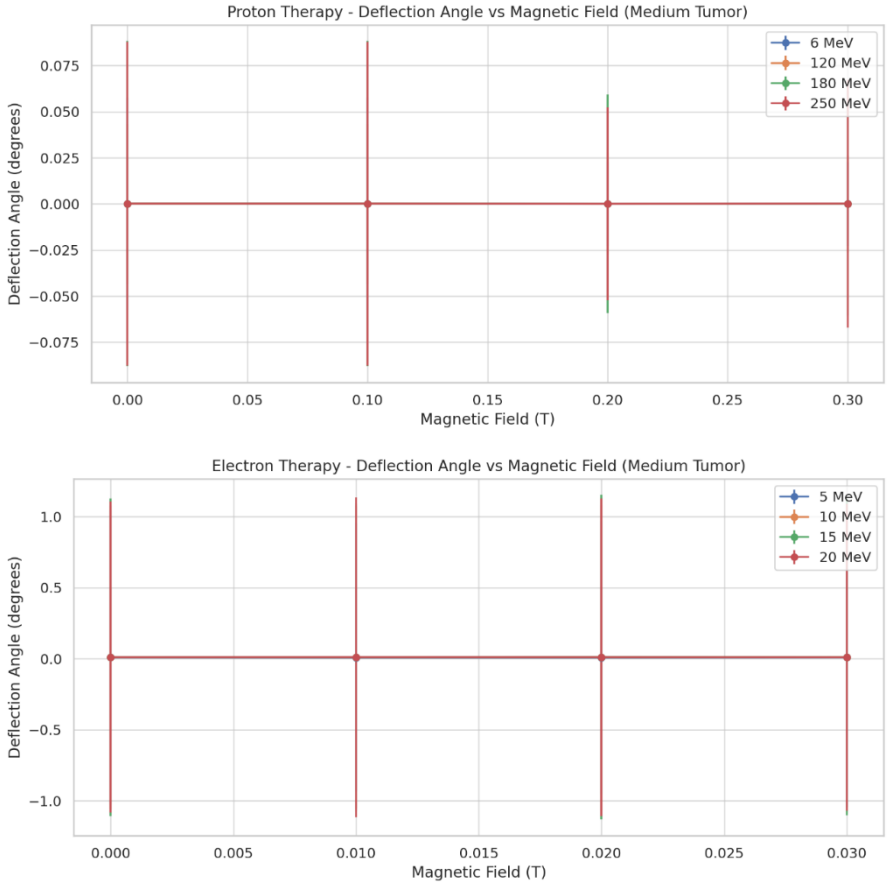

Figure 7. Deflection angle vs magnetic field in the medium depth tumor simulation. In case of proton therapy (top) and electron therapy (bottom).

International Journal of Environmental Sciences
ISSN: 2229-7359
Vol. 11 No. 21s, 2025
https://theaspd.com/index.php

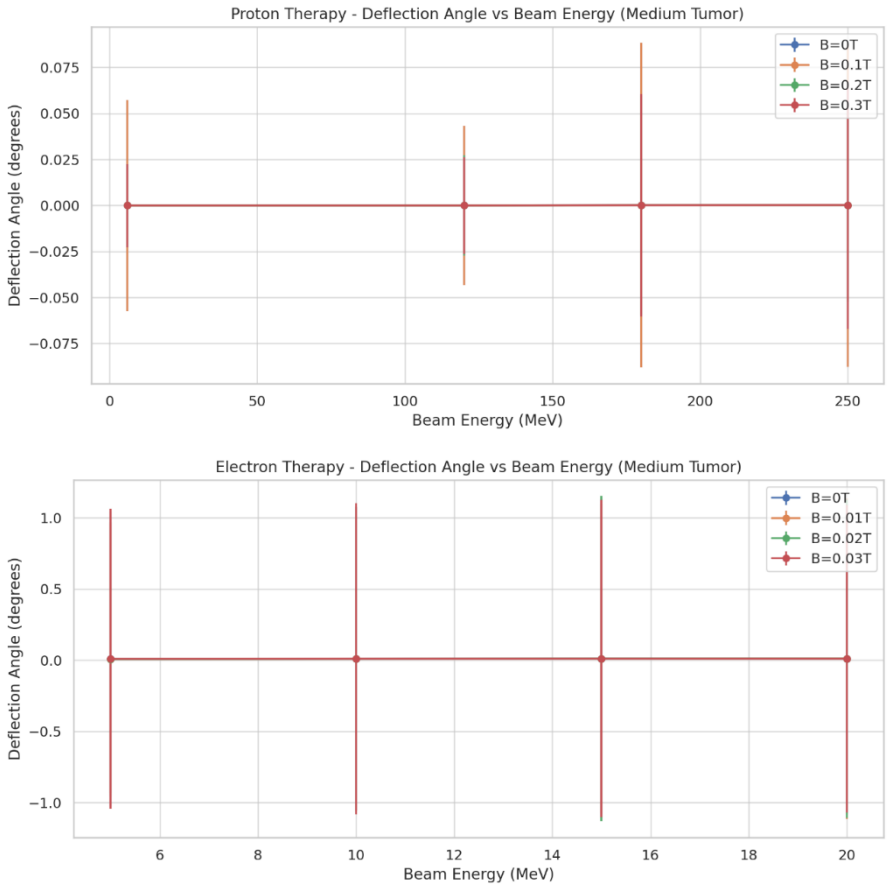

Figure 8. Deflection angle vs beam energy in the medium depth tumor simulation. In case of proton therapy (top) and electron therapy (bottom).

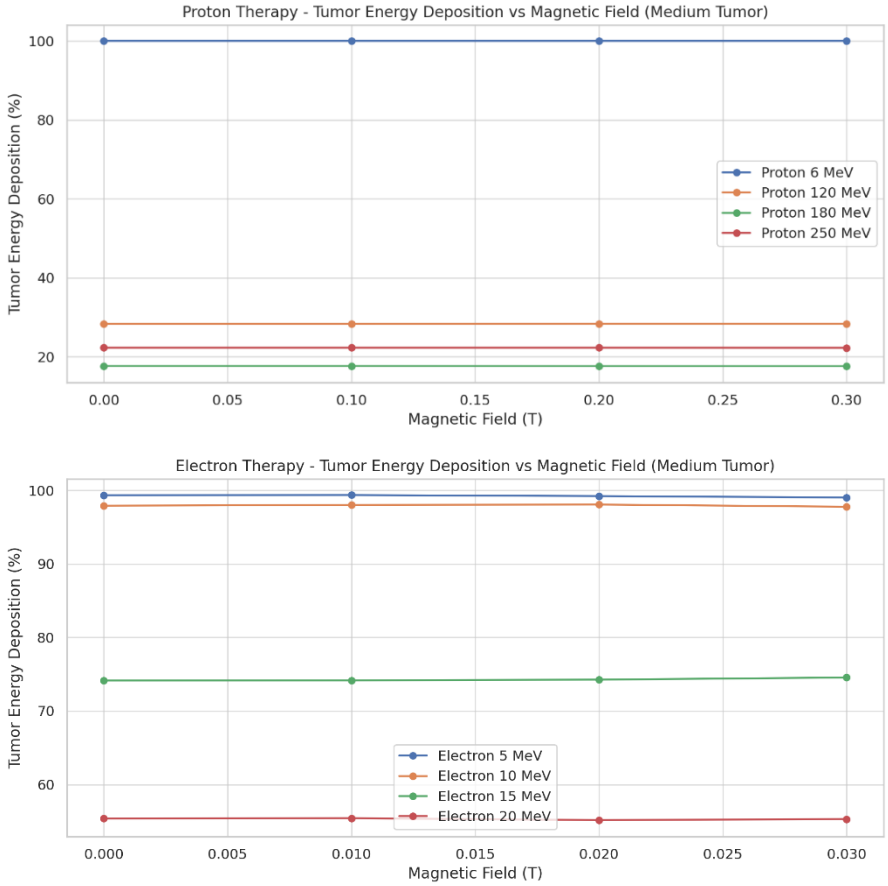

Figure 9. Tumor energy deposition vs magnetic field in the medium depth tumor simulation. In case of proton therapy (top) and electron therapy (bottom).

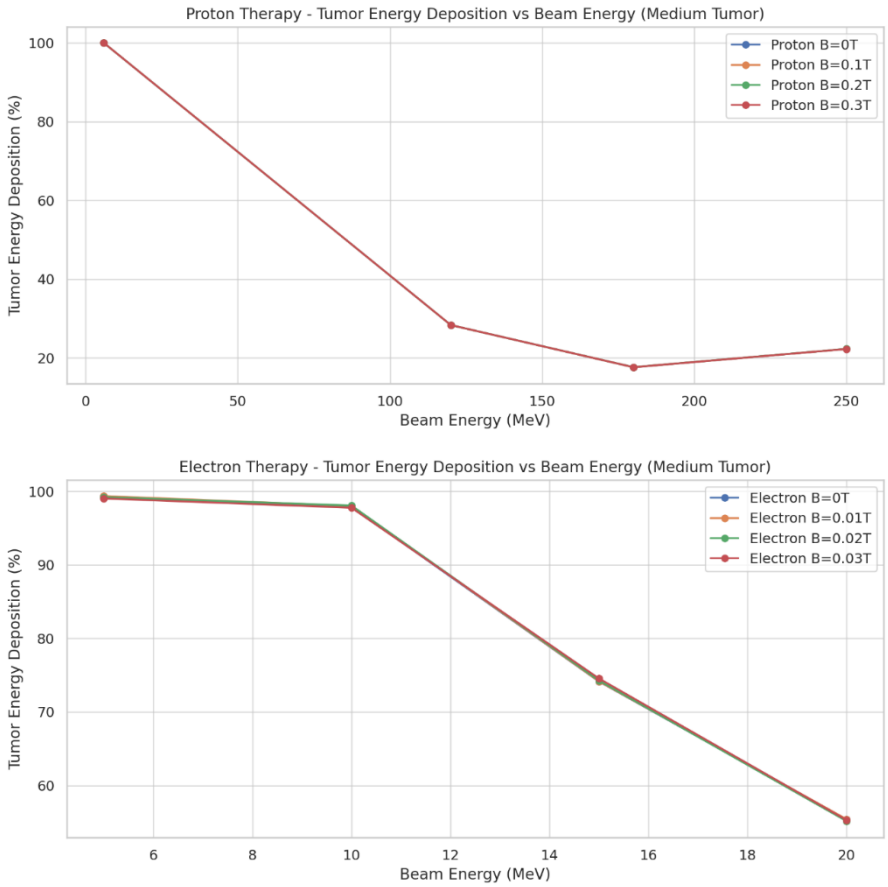

Figure 10. Tumor energy deposition vs beam energy in the medium depth tumor simulation. In case of proton therapy (top) and electron therapy (bottom).

3.3 Deep Tumor

Table 3 shows the collected data from Geant4 in case of medium depth tumor of thickness 2 cm placed 10 cm away from the surface of a water phantom.

TABLE 3. DEEP TUMOR SIMULATION RESULTS.

Deep Tumor							
Magnetic Field (Tesla)	Beam Energy (MeV)	Pre-Tumor Energy Deposit (MeV)	Tumor Energy Deposit (MeV)	Post-Tumor Energy Deposit (MeV)	Deflection Angle (degree)		Tumor Percentage Energy Deposit (%)
					Mean	SD	
Electron Therapy							
0	5	1079.3400	1.2273	2.2726	0.0088	1.0147	0.11%
	10	2075.8500	4.3474	16.5198	0.0000	0.0110	0.21%
	15	3050.9600	16.4985	32.6396	0.0000	0.0106	0.53%
	20	3902.8500	30.5102	74.0141	0.0000	0.0105	0.76%
0.01	5	1080.9100	1.5428	2.2520	0.0000	0.0078	0.14%
	10	2079.1400	3.7993	14.5384	0.0000	0.0109	0.18%
	15	3050.5000	16.0577	34.7225	0.0000	0.0113	0.52%
	20	3897.5500	34.7006	67.6826	0.0000	0.0103	0.87%
0.02	5	1078.6400	2.0138	3.3356	0.0000	0.0076	0.19%
	10	2079.4100	3.8929	14.2985	0.0000	0.0102	0.19%
	15	3044.5200	18.0316	33.1611	0.0000	0.0108	0.58%
	20	3900.1500	33.4164	67.0381	0.0000	0.0105	0.84%
0.03	5	1080.1900	1.3368	3.8852	0.0000	0.0093	0.12%

	10	2078.2200	6.5163	15.0975	0.0000	0.0109	0.31%
	15	3044.1700	15.9617	32.5239	0.0000	0.0108	0.52%
	20	3909.4600	31.9164	68.7511	0.0000	0.0101	0.80%
Proton Therapy							
0	6	16654.2000	0.0000	0.0000	0.0000	0.0000	0.00%
	120	24207.7000	7453.6500	0.0333	0.0000	0.0000	23.54%
	180	13227.6000	3426.7600	18423.6000	0.0000	0.0001	9.77%
	250	9940.1800	2315.7000	9393.8600	0.0000	0.0002	10.70%
0.1	6	16654.2000	0.0000	0.0000	0.0000	0.0000	0.00%
	120	24213.8000	7452.8700	0.0680	0.0000	0.0000	23.54%
	180	13228.6000	3427.6800	18435.0000	0.0000	0.0001	9.77%
	250	9935.3700	2313.3200	9392.0800	0.0000	0.0001	10.69%
0.2	6	16654.3000	0.0000	0.0000	0.0000	0.0000	0.00%
	120	24222.3000	7447.3200	0.0036	0.0000	0.0000	23.52%
	180	13229.0000	3427.1100	18441.0000	0.0000	0.0001	9.76%
	250	9936.5100	2315.3300	9395.0400	0.0000	0.0002	10.70%
0.3	6	16654.2000	0.0000	0.0000	0.0000	0.0000	0.00%
	120	24231.8000	7433.7100	0.0398	0.0000	0.0000	23.48%
	180	13233.9000	3436.3900	18471.6000	0.0000	0.0001	9.78%
	250	9940.6200	2316.6600	9401.3600	0.0000	0.0002	10.70%

For deep-seated tumors and as seen in figures 11-14, electron therapy proved highly ineffective, with tumor deposition percentages below 1% across all energy and magnetic field combinations. Most energy was absorbed in pre-tumor regions (up to ~3900 MeV), with substantial scatter and loss before reaching the tumor.

Magnetic fields had no significant effect on deflection angle or depth penetration at these energies, confirming that electrons should be avoided for deep-target applications unless tissue thickness is minimal.

Protons provided moderate dose delivery to deep tumors at energies ≥120 MeV, with tumor energy deposition peaking around 7453.65 MeV. Unlike electrons, proton energy was distributed more favorably across the pre-tumor and tumor regions, with controllable post-tumor spillover.

Average deflection angles remained negligible (up to 0.0002°) even at 250 MeV, affirming robust trajectory fidelity. This confirms the role of proton therapy as the preferred choice for deep tumor irradiation, especially in complex geometries.

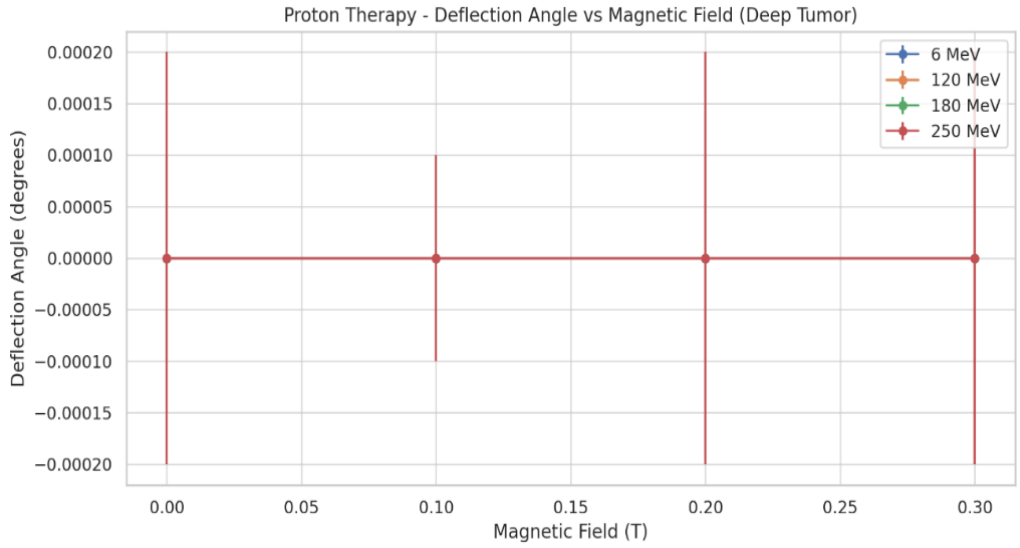

International Journal of Environmental Sciences
ISSN: 2229-7359
Vol. 11 No. 21s, 2025
https://theaspd.com/index.php

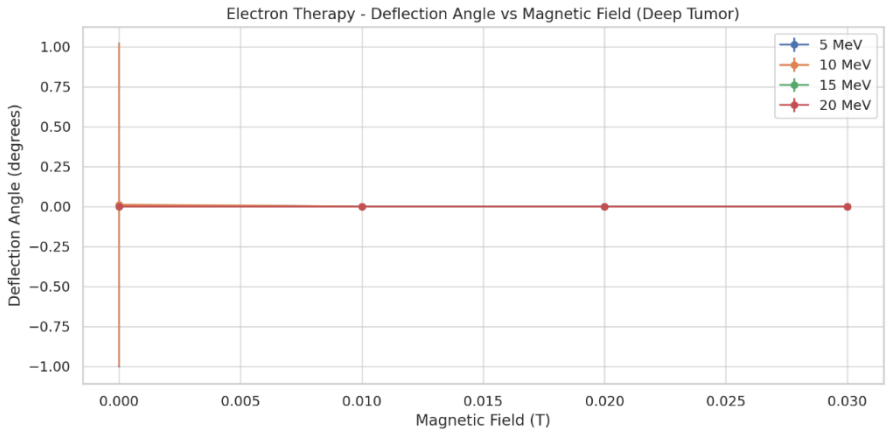

Figure 11. Deflection angle vs magnetic field in the deep tumor simulation. In case of proton therapy (top) and electron therapy (bottom).

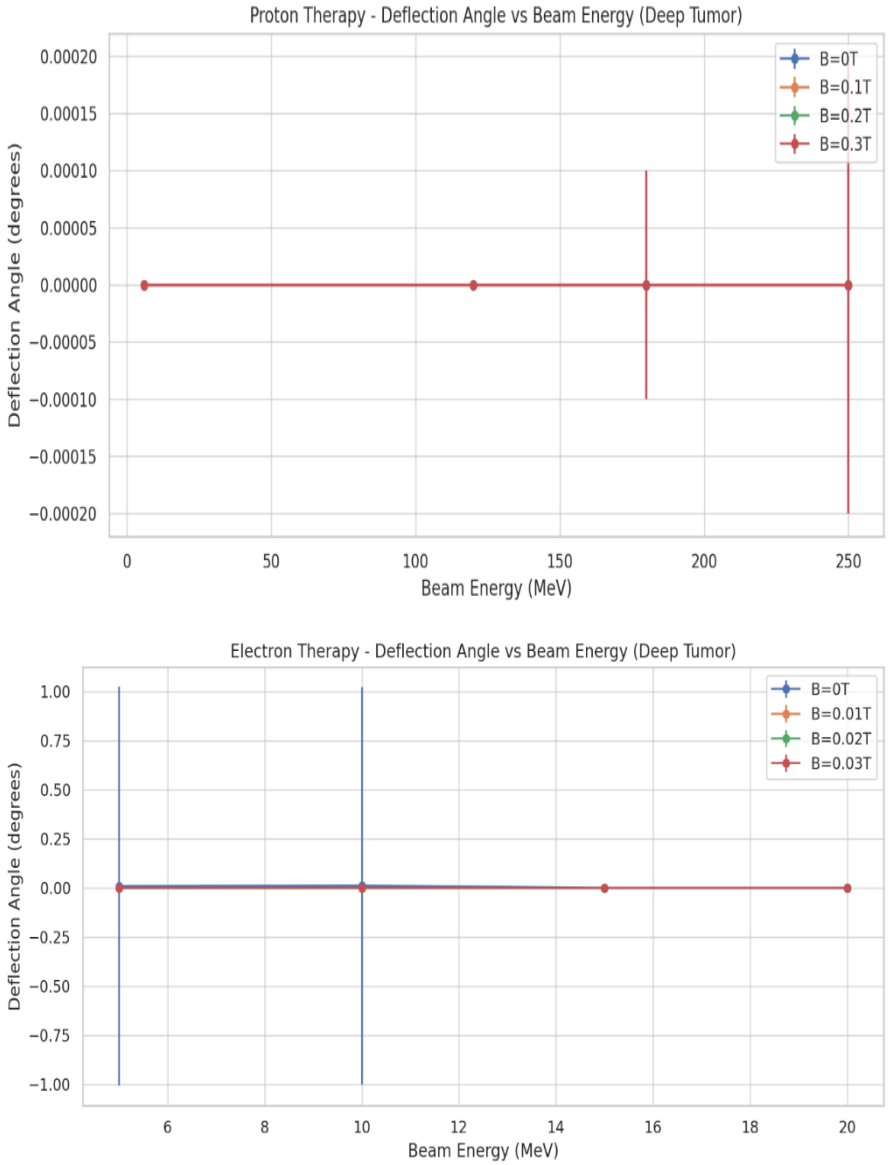

Figure 12. Deflection angle vs beam energy in the deep tumor simulation. In case of proton therapy (top) and electron therapy (bottom).

International Journal of Environmental Sciences
ISSN: 2229-7359
Vol. 11 No. 21s, 2025
https://theaspd.com/index.php

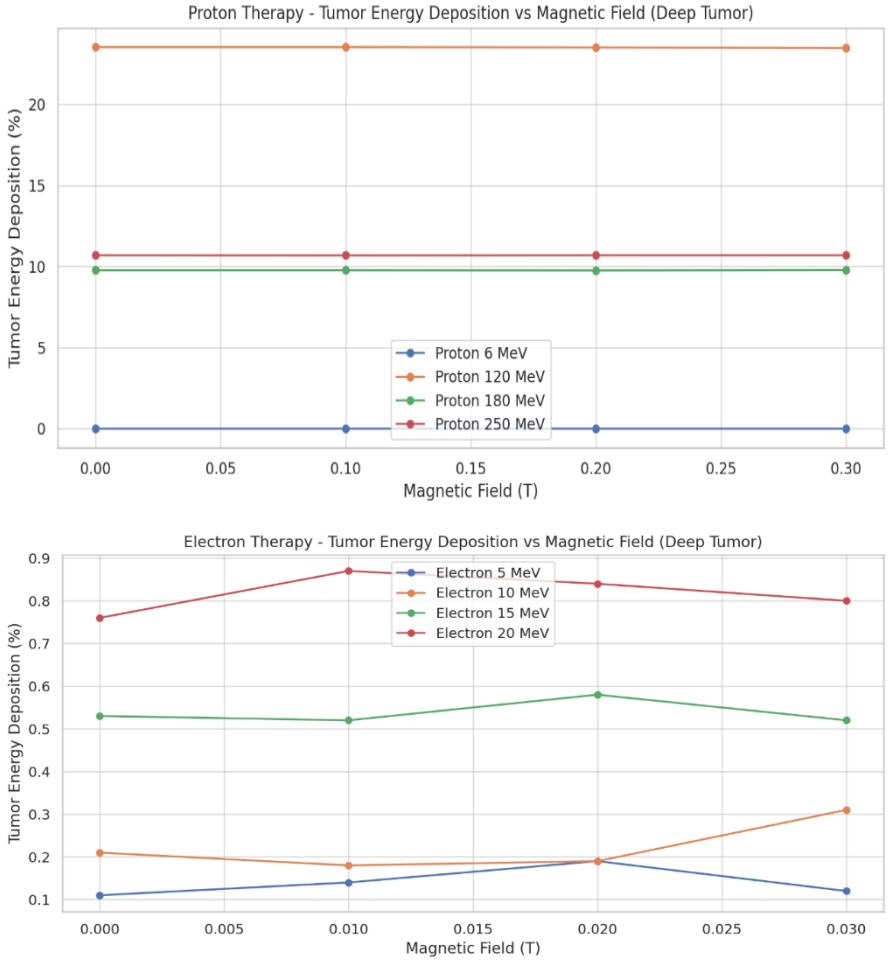

Figure 13. Tumor energy deposition vs magnetic field in the deep tumor simulation. In case of proton therapy (top) and electron therapy (bottom).

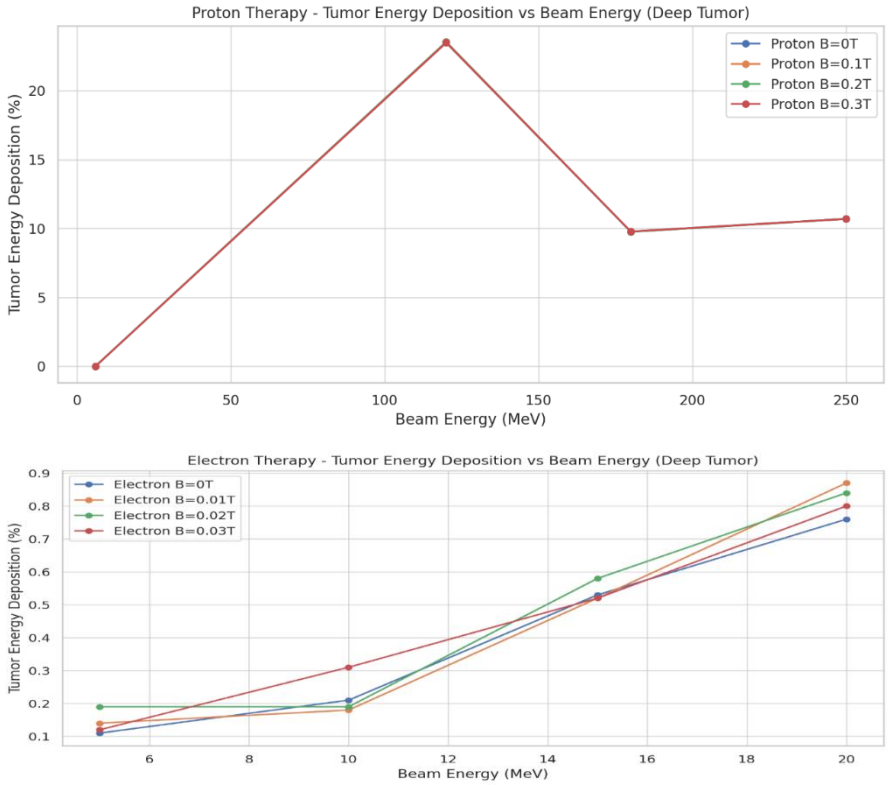

Figure 14. Tumor energy deposition vs beam energy in the deep tumor simulation. In case of proton therapy (top) and electron therapy (bottom). In case of proton therapy (top) and electron therapy (bottom).

IV. DISCUSSION

This study presents a comprehensive Monte Carlo simulation-based analysis using Geant4 to evaluate and compare the performance of electron and proton therapy in terms of energy deposition, spatial precision, and sensitivity to magnetic fields. The simulations covered three clinically relevant tumor depths—shallow, medium, and deep—with a broad range of beam energies and magnetic field strengths. Detailed scoring of energy deposition in pre-tumor, tumor, and post-tumor regions provided a clear and quantitative understanding of each modality's behavior under realistic clinical conditions. The study findings can be concluded in the following:

Electron Therapy is highly effective for shallow and moderately deep tumors, delivering up to 99.4% of the energy within the tumor region at low to intermediate energies (5–15 MeV). However, electrons rapidly lose efficacy for deep tumors due to significant scattering, rapid energy dissipation, and poor penetration beyond 2–3 cm. The simulations clearly demonstrated that for deep tumors, the tumor region receives less than 1% of the total deposited energy.

Proton Therapy, in contrast, showed excellent adaptability across all tumor depths. Low-energy protons (6 MeV) were optimal for shallow tumors, concentrating nearly all the dose within the target. As beam energy increased (up to 250 MeV), protons maintained relatively focused energy deposition across medium and deep tumors, with tumor doses reaching up to 9450 MeV. The Bragg peak behavior of protons enabled sharp distal dose falloff, minimizing damage to healthy tissue beyond the target.

Magnetic Field Effects varied significantly between the two modalities. Electrons, due to their lower mass and higher charge-to-mass ratio, experienced greater deflection in transverse magnetic fields, with angles reaching 0.0123°. Proton beams, by comparison, exhibited deflection angles as small as 0.0001°, maintaining trajectory stability even under fields up to 0.3 T.

Across all tumor depths, proton therapy consistently outperformed electron therapy in energy delivery to deep-seated targets and offered better control of post-tumor dose with the aid of magnetic steering. Electron therapy, however, remains superior for treating surface-level lesions, due to its sharp entrance dose and minimal infrastructure requirements.

Across all simulations, Electrons showed consistent increases in deflection angle with stronger fields but negligible changes in tumor deposition. Protons were minimally deflected due to greater mass, but the magnetic field improved beam shaping and exit dose control. Proton deflection angles were orders of magnitude smaller than electrons (10^{-4}° vs 10^{-2}°), highlighting their higher spatial precision.

These results underscore the importance of tailoring beam energy and magnetic field to tumor depth and location. While electrons remain highly effective for superficial treatments, their utility decreases drastically with depth. Proton therapy, by contrast, offers depth-selective precision and minimal deflection under strong magnetic fields, making it highly suitable for deep and sensitive anatomical regions.

V. CONCLUSION

The results of this study have direct clinical significance in guiding the modality selection and beam parameter optimization for tumor-specific treatment planning as for superficial tumors, electron therapy is both effective and cost-efficient, with high tumor dose percentages and manageable magnetic deflection. Minimal magnetic field corrections are needed, and treatment is accessible even in low-resource environments. While for intermediate or deep-seated tumors, proton therapy offers significant advantages, particularly in terms of dose conformity and magnetic field tolerance. The findings affirm its superiority in treating tumors near critical organs where dose control and spatial accuracy are paramount. The use of magnetic fields as a steering or modulation tool is promising, especially for proton therapy.

While the simulations offer valuable insights, several limitations must be acknowledged, such as that, the simulations were performed on water-equivalent phantoms and idealized geometries, which may not fully capture real human body interactions with charged particles. In addition, to build on these results, we recommend using anatomically realistic phantoms and patient-specific imaging data.

In conclusion, this work demonstrates the critical importance of matching particle type and beam parameters to tumor characteristics. It confirms that electron therapy is highly effective for shallow targets, while proton therapy provides superior control and versatility for deep or anatomically sensitive tumors. The role of magnetic fields is particularly beneficial in proton beam shaping and dose localization. These findings support patient-specific treatment planning strategies that leverage the unique advantages of each modality to maximize clinical outcomes and minimize complications.

REFERENCE

[1] PAGANETTI, Harald. Proton Beam Therapy. Bristol: IOP Publishing, 2017.
[2] Paganetti, H. (Ed.). (2018). Proton Therapy Physics (2nd ed.). CRC Press. https://doi.org/10.1201/b22053
[3] Mohan, R., & Grosshans, D. (2017). Advanced Drug Delivery Reviews, 109, 26–44. https://doi.org/10.1016/j.addr.2016.11.006
[4] Mohan, R. (2022). Precision Radiation Oncology, 6(2), 164–176. https://doi.org/10.1002/pro6.1149
[5] Newhauser, W. D., & Zhang, R. (2015). Physics in Medicine and Biology, 60(8), R155–R209. https://doi.org/10.1088/0031-9155/60/8/r155
[6] Lim, D. H. (2018). Journal of Korean Neurosurgical Society, 61(3), 386–392. https://doi.org/10.3340/jkns.2018.0004
[7] Tahmasebi Birgani, M. J., et al. (2017). Electronic Physician, 9(12), 5932–5939. https://doi.org/10.19082/5932
[8] Sanny, J., Moebs, W., & Ling, S. J. (2016). University Physics: Volume 2.
[9] Pham, T. T., et al. (2022). Radiotherapy and Oncology. https://doi.org/10.1016/j.radonc.2022.02.031
[10]Agostinelli, S., et al. (2003). Nuclear Instruments and Methods in Physics Research Section A, 506(3), 250–303. https://doi.org/10.1016/s0168-9002(03)01368-8
[11]Pratiyogita Darpan. (2002). Competition Science Vision, 2(22).
[12]Griffiths, D. J. (1999). Introduction to Electrodynamics (3rd ed.). Prentice Hall.
[13]Dewar, J. M., & Zill, D. G. (2011). Precalculus with Calculus Previews. Jones & Bartlett.
[14]Internal simulation data from: Geant4 Study of Proton Deflection and Geant4 Study of Electron Deflection, IMSIU, May 2025.